

ADVANCED MATERIALS

Supporting Information

for *Adv. Mater.*, DOI: 10.1002/adma.201502771

Soft Poly(dimethylsiloxane) Elastomers from Architecture-
Driven Entanglement Free Design

*Li-Heng Cai, Thomas E. Kodger, Rodrigo E. Guerra, Adrian
F. Pegoraro, Michael Rubinstein,* and David A. Weitz**

DOI: 10.1002/ adma.201502771

Article type: Communication

Supporting Information

Soft Polydimethylsiloxane Elastomers from Architecture-driven Entanglement Free Design

Li-Heng Cai^{1†}, Thomas E. Kodger^{1†}, Rodrigo E. Guerra¹, Adrian F. Pegoraro¹, Michael Rubinstein^{2*}, and David A. Weitz^{1*}

¹School of Engineering and Applied Sciences, Harvard University, Cambridge, MA 02138, USA.

²Department of Chemistry, University of North Carolina, Chapel Hill, NC 27599-3290, USA.

[†]The first two authors (Cai and Kodger) contributed equally to this work.

*Correspondence and requests for materials should be addressed to: D.A.W., weitz@seas.harvard.edu or M.R., mr@unc.edu

Supporting Information:

SI Text

SI Methods

Figures S1-S12

Table S1

SI Movies

SI Text

S1. Entanglement molecular weight of bottlebrush polymers. Consider a bottlebrush molecule with backbone of N_{bb} Kuhn monomers and side chain of N_{sc} Kuhn monomers. The side chains are densely grafted to the backbone polymer, occupying the cylindrical space surrounding the backbone polymer. The cross section of the cylindrical space is about the size R_{sc} of a side chain; it increases as the distance d along the backbone between two neighboring grafting sites decreases. However, the volume occupied by a side chain v_{sc} is constant; it is determined by the number of monomers per side chain: $v_{sc} = N_{sc}v_0$, in which v_0 is the volume of a Kuhn monomer. This side chain fills the volume R_{sc}^2d , which is the space available for it within the cylindrical volume of the bottlebrush. Therefore, the size of a side chain is

$$R_{sc} = \left(\frac{N_{sc}v_0}{d} \right)^{1/2} \quad (S1)$$

suggesting the cross section of the bottlebrush molecule increases with the grafting density $1/d$ along the backbone.

Such a bottlebrush molecule can be considered a “fat” linear polymer, with *effective* monomer size, b_{eff} , on the order of the cross section of size R_{sc} of the bottlebrush molecule. An *effective* monomer contains $n_{sc} = R_{sc}/d$ side chains. Therefore, the total number of Kuhn monomers in an *effective* monomer is $N_{eff} = n_{sc}N_{sc} + R_{sc}/b$, in which b is the spacing between backbone monomers along its contour and R_{sc}/b counts for the number of Kuhn monomers of a section of stretched backbone polymer with size R_{sc} . Recalling equation (S1) one obtains the number of Kuhn monomers per *effective* monomer:

$$N_{eff} = \frac{N_{sc}R_{sc}}{d} + \frac{R_{sc}}{b} \approx N_{sc}^{\frac{3}{2}} \left(\frac{v_0}{d^3} \right)^{1/2} \quad (S2)$$

in which we drop the second term, corresponding to the number of backbone monomers, as typically it is much smaller compared to the contribution from side chains for a densely grafted bottlebrush molecule.

The increase in size of an *effective* monomer compared to a Kuhn monomer suggests that the ‘fat’ linear polymer becomes relatively stiffer^[1]. To estimate the entanglement molecular weight for the ‘fat’, bottlebrush polymer, we use the Kavassalis & Noolandi conjecture^[1]: The number of entanglement strands in the volume pervaded by an entanglement strand is assumed to be constant $P \approx [b_{eff} n_e^{1/2}]^3 / (b_{eff}^3 n_e)$, in which n_e is the number of *effective* monomers per entanglement strand, $[b_{eff} n_e^{1/2}]^3$ represents the volume pervaded by an entanglement strand of size $b_{eff} n_e^{1/2}$, and $b_{eff}^3 n_e$ corresponds to the volume of an entanglement strand. Therefore, the number of *effective* monomers per entanglement strand is: $n_e \approx P^2$. Recall equation (S2) for the number of Kuhn monomers per *effective* monomer, one obtains the number of Kuhn monomers per entanglement strand the ‘fat’, bottlebrush molecule:

$$N_e \approx n_e N_{eff} \approx P^2 N_{sc}^{3/2} \left(\frac{v_0}{d^3} \right)^{1/2} \quad (S3)$$

To use equation (S3) for experimental conditions, one can estimate the entanglement molecular weight of bottlebrush molecules by using the mass of a PDMS Kuhn monomer $M_0 = 381$ g/mol^[2]. Thus, the number of Kuhn monomers per *side chain* of the molecular weight 4,750 g/mol utilized in this work is $N_{sc} \approx 13$. The *backbone* polymer is a copolymer of molecular weight 50,000 g/mol that contains ~600 chemical units. However, only about half of the *backbone* monomers are reactive vinyl groups. Thus, there are about 300 reactive vinyl groups on the *backbone* polymer. In addition, during the fabrication of soft PDMS elastomers, we use only half of the reactive sites to graft *side chains*. Therefore, the distance d between two neighboring grafting sites along the contour of backbone polymer is about the

length of four PDMS chemical units. The length l of a chemical unit for PDMS (Si-O) bond is 1.64×10^{-1} nm, which gives $d=4l=6.56 \times 10^{-1}$ nm; this value is smaller than 1.3 nm, the length of a Kuhn monomer of PDMS, and thus the backbone polymer is almost fully stretched. The volume of a PDMS Kuhn monomer is $v_0 = 6.50 \times 10^{-1} \text{ nm}^3$ [2, 3]. For a typical value of $P=20$, the number of PDMS Kuhn monomers per entanglement strand of a “fat” bottlebrush molecule is (equation S3): $N_e \approx 20^2 \times 13^{3/2} \left(\frac{6.50 \times 10^{-1} \text{ nm}^3}{3.28^3 \times 10^{-3} \text{ nm}^3} \right)^{1/2} \approx 8.0 \times 10^5$. Thus, the entanglement molecular weight of the bottlebrush molecule is

$$M_e \approx N_e M_0 \approx 3.0 \times 10^7 \text{ g/mol} \quad (\text{S4})$$

which is more than one order of magnitude larger than the molecular weight of the bottlebrush molecule, $\sim 10^6$ g/mol, for soft PDMS elastomers. Importantly, this entanglement molecular weight of the bottlebrush molecule suggests a lower limit of the modulus for soft elastomers for this set of parameters; the modulus can reach $G=k_B T \rho / M_e \sim 100 \text{ Pa}$ by using longer backbone polymers. In addition, increasing the molecular weight of side chain by the factor of three will result in even lower modulus, $3^{-3/2} \times 100 \text{ Pa} \sim 10 \text{ Pa}$, if “impurities”, di-functional crosslinking chains, in mono-functional side chains were removed.

S2. Entanglement concentration of backbone polymers. The long, linear *backbone* polymer has a molecular weight of 50,000 g/mol, above the entanglement molecular weight $M_e=12,000$ g/mol of linear PDMS polymers in melts [2]. Therefore, the backbone polymers may form entanglements before polymerization; however, they are heavily diluted by relatively short, unentangled side chains. These short side chains and long backbone molecules form a bi-disperse melt. In such a melt, the conformation of backbone polymers are random coil-like, with size proportional to the molecular weight of power 1/2, as long as the degree of polymerization of long backbone molecules is smaller than the square of the short

side chains^[2]. Recent studies suggest a small correction to the size of a long polymer in a melt of short polymers due to chain connectivity.^[4] The correction is less than 3% for our system and for simplicity we ignore this correction in our estimate and assume that the conformation of the backbone polymer is ideal-like. The entanglement volume fraction ϕ_e of the long backbone polymer in a bi-disperse melt is: $\phi_e \approx [N_e(1)/N_{bb}]^{3/4}$,^[2] in which $N_e(1) = 32$ is the number of Kuhn monomers per entanglement strand for PDMS in a melt, $N_{bb} = 131$ is the number of Kuhn monomers per backbone polymer. Therefore, the entanglement volume fraction for linear backbone polymer is: $\phi_e \approx 0.35$, which is about 6 times higher than the largest volume fraction $\phi_{bb} \sim 0.06$ used to fabricate the soft PDMS elastomers. Thus, the long, linear backbone polymers are not entangled neither before nor after polymerization.

S3. Modulus of an unentangled polymer network. The elastic modulus of an unentangled polymer network is $G = k_B T(\nu - \mu)$, in which ν is the number density of *elastically effective* network strands and μ is the number density of elastically effective crosslinks^[5]. Here elastically effective network strands or crosslinks are the ones that can bear stress. For instance, the dangling chains and their crosslinks are not elastically effective.

To estimate the number density of elastically effective crosslinks and network strands in our soft elastomers, we consider the case in which the molar ratio between *backbone* polymers and *crosslinking chains* is $1:n_{cl}$, as shown in **Figure S3**. A fully reacted, bridging crosslinking chain contributes 2 elastically effective crosslinks, as shown by two dashed circles in **Figure S3**. The addition of 2 crosslinks to backbone polymers adds 2 more polymer sections, and thus results in 3 more elastically effective network strands, taking into account that the crosslinking chain itself is elastically effective as well. However, the two crosslinks from the first crosslinking chain divide the backbone polymer into three sections, leaving two

dangling chains; thus, they contribute only 2 elastically effective network strands. Therefore, for a bottlebrush molecule with on average n_{cl} crosslinking chains, there are $3n_{cl} - 1$ elastically effective network strands and $2n_{cl}$ elastically effective crosslinks. Thus, the modulus of the elastomer is

$$G = k_B T \frac{(n_{cl}-1)}{M/\rho} \quad (S5)$$

in which $\rho=0.97 \text{ g/cm}^3$ is the density of PDMS and M is the mass of the bottlebrush molecule that includes a backbone polymer, side chains, and crosslinking chains.

S4. Quantification of the fraction of “impurities” in extension chains. The chain extension polymer is a monovinyl-monohydride terminated polydimethylsiloxane, which has molecular weight of 10,000 g/mol with two ends functionalized differently, one carrying a vinyl group while the other carrying a hydride group. Only the hydride group can react with the vinyl groups on the backbone polymer. Therefore, in principle the PDMS-catalyst mixture that contains only *backbone polymers* and *extension chains* will not form a network due to lacking of di-functional crosslinking chains that have a hydride group at both ends. However, we observe a finite shear storage modulus for the polymerized PDMS-catalyst mixture that contains *backbone polymers* and *chain extensions* with number ratio of 1:150, as shown in **Figure S6**. This suggests there are “impurities” – crosslinking chains – in the commercially available *extension chains*. The shear modulus of the elastomer $G=6760\text{Pa}$ allows us to estimate the fraction of “impurities” on the basis of equations (S5) or (1): $f_{ip}^{ext}=[GM/(\rho k_B T)+1]/n_{ext}=3.54 \times 10^{-2}$, in which $n_{ext}=150$ is the number of *extension chains* per bottlebrush molecule, $M=1.55 \times 10^6 \text{ g/mol}$ is the molecular weight of the bottlebrush molecule, $\rho=0.97 \text{ g/cm}^3$ is the density of PDMS, k_B is Boltzmann constant, and $T=293\text{K}$. Therefore, the number of effective crosslinking chains per bottlebrush molecule for sample **SEL**, molar ratio backbone: side chain: extension chain = 1:150:150, is

$n_{cl}^{eff} = f_{ip}^{ext} \times 150 + f_{ip}^{ex} \times 150 = 9$, in which $f_{ip}^{ext} = 3.54 \times 10^{-2}$ and $f_{ip}^{sc} = 2.56 \times 10^{-2}$ Considering the mass, $M=2.2 \times 10^6$ g/mol, for a bottlebrush molecule, and the “impurities” contained in both side chains and extension chains, the predicted modulus, $G=2400\text{Pa}/(10^6\text{g/mol}) (n_{cl}^{eff}-1)/M=8600$ Pa, agrees reasonably well with the measured value 7500 Pa.

S5. Properties of commercial silicone products. Sylgard[®] 184 is one of the most widely used kits for producing PDMS elastomers. The fabrication of Sylgard[®] PDMS elastomers involves simply mixing the base agent, a mixture of divinyl functional PDMS polymers and Platinum catalyst, and a curing agent that contains crosslinkers, then polymerizing the mixture at 65°C for >6 hours. The polymerized product has a shear storage modulus of ~1 MPa for a typical curing-agent/base mass ratio of 1:10. The gel fraction of the 1:10 Sylgard[®] PDMS elastomer is ~96% (wt/wt) (**Table S1**). To achieve lower moduli, the cure agent/base ratio must be decreased such that the concentration of crosslinking molecules decreases. However, the gel fraction in Sylgard[®] PDMS elastomers decreases significantly as their moduli becomes smaller. For instance, the Sylgard[®] PDMS elastomer with $G \sim 4$ kPa, with curing agent/base ratio 1:50, has only about 50% gel fraction; moreover, the gel fraction becomes negligible, <2%, when the modulus approaching ~1 kPa, as listed in **Table S1**. The shear storage modulus of such Sylgard[®] PDMS elastomers increases by an order of magnitude as the oscillatory shear frequency increases from 10^{-3} Hz to 10^2 Hz for the sample with curing agent/base ratio 1:50; moreover, the shear loss modulus for this sample becomes comparable to the storage modulus at high frequency 10^2 Hz, as shown in **Figure S7A**.

Dow Corning CY 52-276 is a commonly used soft silicone product. The preparation of this silicone gel is similar to that of Sylgard[®] 184, by mixing part A and part B with mass ratio at 1:1, and curing at 70°C for 1hr. The polymerized sample has a shear modulus of ~1

kPa and a low gel fraction, 59% (wt/wt) (**Table S1**). The behavior of this silicone product is reminiscent of a viscoelastic gel; both the storage and loss moduli rapidly increase with shear frequency with the magnitude of loss modulus becoming comparable to that of the storage modulus at relatively high shear frequency, as shown in **Figure S7B**.

S6. Behavior of loss modulus for soft PDMS elastomers. The loss modulus for soft PDMS elastomer is very small, nearly two orders of magnitude smaller than that of storage modulus. Nevertheless, it is clearly measurable, and exhibits a power-law dependence on frequency: $G''(\omega) \sim \omega^\alpha$. Remarkably, the value of the exponent α exhibits a strong dependence on the network elastic modulus; it increases from ~ 0.3 to ~ 0.7 as the elastic modulus decreases from ~ 100 kPa to ~ 10 kPa in the frequency range of 0.1 - 100 Hz, as shown by the empty symbols in **Figure 2B**. At time scales corresponding to this frequency range, most precursor chains and network strands have already relaxed. To understand the behavior of loss modulus, one needs to consider dangling polymers that relax at longer time scales.

S6.1. Formation of long dangling polymers. In soft PDMS elastomers, the long dangling polymers are produced by the reaction between di-functional chains and multi-functional molecules. For instance, a reactive site on a multi-functional molecule can react with one end of a di-functional chain, and the other end of this di-functional chain can attach to the network framework. This reaction results in the formation two dangling ends if the rest reactive sites on the bottlebrush molecule remain unreacted, as shown in **Figure S8A**. The dangling ends are not necessarily linear, but could have branch points. For instance, a dangling end can have other multi-functional molecules connected to it, forming a branched structure. However, for a network formed by randomly crosslinking multifunctional polymers, the probability of forming dangling ends with branch points is very small at high concentration of crosslinks; it is more likely for a secondary dangling end to attach to the network framework rather than being unreacted with the reactive sites on the backbone polymer. Indeed, the average number

of branch points per dangling end rapidly approaches zero with the increase of crosslinking density.^[6] In our estimate, we therefore consider the dangling ends as linear polymers.

To estimate the size distribution of dangling ends, we introduce the probability of a reactive site on a multifunctional polymer to form a crosslink: $q = 2n_{ct}/r$, in which r is the number of reactive sites per multifunctional polymer, and n_{ct} is the number of di-functional crosslinking chains per multifunctional polymer. The factor 2 comes from the fact that a di-functional crosslinking chain reacts with two sites on the multifunctional polymer. The probability of a given reactive site on a multifunctional polymer being crosslinked is q , and the probability of having consecutive N sites are unreacted is $(1 - q)^N$. Therefore, the probability of having a dangling end with degree of polymerization of N is $p(N) = q(1 - q)^N$. The number average molecular weight of dangling ends is $N_n = \sum Np(N) = 1/q$.

S6.2. Stress relaxation due to dangling polymers. To understand the relaxation of a dangling polymer, we consider the bottlebrush molecule as an effective thick linear polymer, with effective monomer size on the order of that of mono-functional side chains. A thick dangling end is likely to be trapped by network meshes, as shown in **Figure S8B**. Since the dangling polymer cannot physically cross the confining meshes, it has to retract its dangling end from network meshes to relax, a mechanism called arm retraction. During arm retraction, the dangling end sequentially escapes from constraining network meshes; a step of such relaxation process is illustrated in **Figure S8C**. The relaxation dynamics due to arm retraction is exponentially slow^[7]; indeed, it is reminiscent to overcoming free energy barriers that increases with the number of constraining meshes that the dangling end has to escape from.

To understand the effect of relaxation of dangling ends on loss modulus, we consider the stress due to a dangling branched polymer at a certain time scale. To do so, we consider a dangling end of size N . At a certain time scale t , the part of dangling end that has already

relaxed is: $s(t) \approx \gamma N_x \ln\left(\frac{t}{\tau_1}\right)$, in which N_x is the degree of polymerization of a network strand, γ is a constants, and τ_1 is the characteristic relaxation time of the network. The stress due to the dangling chain is proportional to the length of the polymer section that has not yet relaxed. Summing the contribution from all dangling ends gives the time dependent part of the relaxation modulus: $G(t) - G_0 \approx (1/N_x) \sum_{N=s}^{\infty} [N - s(t)] p(N)$, in which $p(N)$ is the probability of having a dangling end of size N .

Recall the size distribution of dangling ends, $p(N) = q(1 - q)^N$, the time dependent network relaxation modulus is

$$\begin{aligned}
 G(t) - G_0 &\approx \frac{1}{N_x} \sum_{N=s}^{\infty} [N - s(t)] q(1 - q)^N \\
 &\approx \frac{1}{N_x} \frac{(1-q)}{q} (1 - q)^{\gamma N_x \ln\left(\frac{t}{\tau_1}\right)} \\
 &\approx \frac{1}{q N_x} [\exp(-q)]^{\gamma N_x \ln\left(\frac{t}{\tau_1}\right)} \\
 &\approx \frac{1}{q N_x} \left(\frac{t}{\tau_1}\right)^{-\beta} ; \beta = \gamma q N_x = \gamma N_x / N_n \quad (S6)
 \end{aligned}$$

Here we use the approximation $(1 - q) \approx \exp(-q)$ for $q \ll 1$. Therefore, for a randomly crosslinked network, the network relaxation modulus has a power-law dependence on time, t : $G(t) \sim t^{-\beta}$, in which $\beta \approx N_x / N_n$ with N_x the network mesh size and N_n the number average molecular weight of dangling polymers.^[8] The relaxation modulus with a power-law decay corresponds to a power-law frequency dependence of loss modulus: $G''(\omega) \sim \omega^\alpha$, in which

$$\alpha = \beta - 1 \approx \gamma N_x q - 1 \quad (S7)$$

The physical meaning of the exponent α is reflected by its correlation to the network mesh size and the length of dangling polymers. It is inversely proportional to the average number of constraints per dangling polymer, N_n / N_x . The exponent α is smaller for longer dangling polymers; longer polymers are subjected to stronger constraints from network meshes and have slower relaxation, resulting in smaller a value of α . Similarly, dangling polymers

experience stronger constraints from smaller network meshes have slower relaxation dynamics; consequently, the exponent α for $G''(\omega)$ becomes smaller.

S6.3. Effect of crosslink density. To elucidate the behavior of loss modulus for soft PDMS elastomers at different stiffness, we exploit the correlation of the size of network mesh, N_x , and the size of dangling polymers, N_n , to the network modulus, G . The network modulus is about $k_B T$ per volume of a network strand, $G \approx k_B T / (N_x v_{eff})$, in which N_x the number of effective monomers per network strand, and v_{eff} is the volume of an effective monomer for bottlebrush molecules. Recall equation (S5) for the modulus of soft PDMS elastomers, $G = k_B T \rho (n_{cl} - 1) / M$, one obtains the network mesh size.

$$N_x \approx \frac{N_b}{n_{cl} - 1} \approx N_b / n_{cl} \quad (S8)$$

Here n_{cl} is the number of crosslinking chains per bottlebrush molecule, and N_b is the number of PDMS monomers per bottlebrush molecule given by: $N_b = N_{bb} + N_{sc} n_{sc} + N_{cl} n_{cl}$, in which N_{bb} , N_{sc} , and N_{cl} are the number of monomers per backbone polymer, side chain, and crosslinking chain respectively, and n_{sc} is the number of side chains per bottlebrush molecule. For fabrication of soft PDMS elastomers, we keep the total number of reactive sites carried by both side chains and crosslinking chains constant: $n_{sc} + 2n_{cl} = 150 \ll n_b$, which gives:

$$N_b = N_{bb} + 150 N_{sc} + (N_{cl} - 2N_{sc}) n_{cl} \quad (S9)$$

The value of N_b is nearly a constant and independent of crosslinking density as N_{cl} is about the twice of N_{sc} . Therefore, the network mesh size $N_x \approx N_b / n_{cl}$ is mainly determined by the density of crosslinking chains.

The average molecular weight of dangling polymers depends on both crosslink density and the amount of side chains due to the unique crosslinking process for soft PDMS elastomers. To examine the crosslinking process, let's take a precursor polymer backbone for example. The backbone polymer carries n_b reactive sites (**Figure S9A**); n_{sc} of them is used as grafting sites to attach side chains and the remaining, $r = n_b - n_{sc}$, sites are candidates for

forming crosslinks, termed as crosslinkable sites (**Figure S9B**). $2n_{cl}$ of these crosslinkable sites, are being crosslinked; n_{cl} is the number of crosslinking chains per backbone polymer and the factor 2 comes from the fact that each crosslinking chain reacts with two crosslinkable sites (**Figure S9C**). Therefore, the probability of a crosslinkable site being crosslinked is $q = 2n_{cl}/r$. The average molecular weight of dangling polymers is inversely proportional to the probability of a crosslinkable site being crosslinked: $N_n \approx \frac{1}{q} \sim r/n_{cl}$ (section **S6.1**). Recall the relation between the number of side chains and crosslinking chains, $n_{sc} + 2n_{cl} = 150$, the expression of r can be rewritten as $r = n_b - 150 + 2n_{cl}$. The value of r is larger at higher modulus for soft PDMS elastomers, at which n_{cl} is larger (smaller n_{sc}), as illustrated by **Figure S9D**.

The average number of constraints per dangling polymer

$$N_n/N_x \approx (n_b - 150 + 2n_{cl})/N_b \quad (\text{S10})$$

increases with network crosslink density, as the number of reactive sites n_b per backbone polymer is a constant, and the molecular weight of a bottlebrush molecule is nearly independent of crosslink density. Thus, the exponent α (equation S7) for the power-law dependence of loss modulus on frequency becomes smaller for elastomers of higher modulus.

$$\alpha \approx 2\gamma \frac{N_b}{n_b - n_{sc}} - 1 = 2\gamma \frac{N_b}{n_b - 150 + 2n_{cl}} - 1 \quad (\text{S11})$$

Here N_b is the molecular weight of bottlebrush molecules with typical value of 10^6 Da, n_b is the number reactive sites per backbone polymer with the value of ~ 270 , n_{cl} is the number of crosslinking chains per bottlebrush molecule, with the value ranging from ~ 5 to ~ 60 for different soft PDMS elastomer samples. Consistent with the prediction from equation (S11), the exponent α indeed increases linearly with the number of constraints per dangling end, as shown in **Figure S10**.

The understanding of the dependence of the exponent α on network modulus is further supported by the measurements for samples with sol fraction extracted. Extracting sol fraction

does not alter the distribution of dangling polymers, but decreases the network mesh size. Therefore, dangling polymers experience stronger constraints, resulting in slower relaxation dynamics; consequently, the power-law decay of $G''(\omega)$ becomes weaker. Indeed, the exponent α for soft PDMS elastomer sample **SE5** decreases from 0.70 to 0.65 after the sol fraction extracted, as shown in **Figure S11**.

We would like to stress that the decrease in the value of exponent α at higher network modulus is due to stronger constraints imposed on dangling polymers. This increase in the number of constraints per dangling polymer is due to the unique crosslinking process of soft PDMS elastomers. Both the size of the network mesh and of the length of dangling polymers decreases with the crosslinking density, yet the later decreases slower, due to the presence of side chains in soft PDMS elastomers. Such crosslinking process is in contrast to vulcanization of conventional elastomers, in which typically only two types of precursor polymers, multifunctional and crosslinking polymers are involved. In this case both the network mesh and the length of dangling polymers decrease with the increase of crosslink density in the same manner. The average network mesh size, $N_x \sim 1/n_{cl}$, is inversely proportional to the concentration of crosslinks, and the length of dangling polymers has a similar dependence on crosslink density, $N_n \approx r/n_{cl} \sim 1/n_{cl}$, as the number of reactive sites r is constant determined by the multifunctional polymers. Therefore, the number of constraints per dangling polymer, N_n/N_x , is independent of crosslink density for conventional elastomers. As a result, the value of the exponent α is nearly a constant at different network moduli. Indeed, this understanding is consistent with our experimental observation for two commercial silicone products, both of which has the same exponent for the frequency dependence of loss modulus, $\alpha = 0.5$, whereas the elastic moduli differ by the factor of ~ 5 , as shown in **Figure S7**.

Note that our estimate is based on the approximation that all dangling polymers are almost linear. This approximation is valid for network well above the gelation threshold with high density of crosslinks, $q \gg 1$, and applies to most soft PDMS elastomer samples. For the soft

PDMS elastomer with the lowest modulus, the number of crosslinks per bottlebrush molecule, $q \approx 4$, is close to the gel point $q = 1$. In this case the dangling polymers are more likely to be branched and the effects of these branches on the relaxation of dangling polymers need to be taken into account.

The above description (analysis) also suggests a way to tune the magnitude of loss modulus but without altering its frequency dependence. The key is to keep the same ratio between multi-functional polymers and di-functional polymers, but use longer mono-functional polymers to make thicker bottlebrush molecules. Thicker bottlebrush molecules result in higher volume fraction of network imperfections, resulting in an increase in the magnitude of loss modulus. Indeed, by introducing extension chains, which make the mono-functional polymers three times larger, we successfully increase the magnitude of loss modulus from 60Pa to 200Pa for frequency at 1Hz, while keeping the frequency dependence of loss modulus the same, with exponent $\alpha = 0.75$, as shown in **Figure S5**.

Finally, we would like to emphasize that the power law dependence of loss modulus $G''(\omega)$ is due to the logarithmically slow relaxation of long dangling polymers and their exponentially low concentration. The fraction of such network defects is very small for soft PDMS elastomers, as evidenced by very small values of loss tangent, $\tan \delta = G''/G' \sim 10^{-3}$, at frequency $\omega=1$ Hz.

S7. Effects of sol fraction on properties of soft PDMS elastomers. The loss modulus and adhesiveness of soft PDMS elastomers are mainly determined by network imperfections, which are primarily dangling side chains and unreacted, free polymers. To elucidate the role of sol fraction, free polymers, on the properties of soft PDMS elastomers, we characterize the dynamical-mechanical behavior and adhesiveness for soft PDMS elastomers before and after the sol fraction being extracted.

To extract the sol fraction, we slowly swell the soft PDMS elastomers allowing free molecules to diffuse out, but without the material cracking during the swelling; this subtle balance between swelling and cracking is achieved by carefully adjusting the solvent quality (**SI Methods**). After extraction, the storage modulus of a soft PDMS elastomer increases from 20 kPa to 25 kPa due to the higher density of crosslinks after extraction; this increase is consistent with extraction of 20% (wt/wt) sol fraction. In addition, the slope of loss modulus upon frequency change decreases from 0.70 to 0.65, as shown in **Figure S11**. Consistent with reduced loss modulus after sol extraction, the fracture energy for the soft PDMS elastomer decreases by ~50% compared to the measurements performed on the same sample before extraction. Collectively, these results provide direct evidence that higher sol fraction corresponds to stronger frequency dependence of loss modulus upon frequency change, and larger material adhesiveness.

SI Methods

We prepare about 5 g of soft PDMS mixture (**Materials and Methods**) and cure it at 80°C for 40 hours in a Petri dish-shaped Teflon mold. After cooling down to room temperature, we perform adhesion measurements on the cured sample. The same sample is then immersed in 135 mL acetone for 24 hours. To ensure that the PDMS slab swells slowly without forming cracks, we add *n*-hexane three times, 5 mL per addition, at an interval of 24 hours, such that the final solution contains acetone and *n*-hexane with a volume ratio of 90:10. The 150 mL solution is changed 5 times with an interval of 24 hours. During this period, the soft PDMS slab is lifted off from the Teflon mold with gentle shaking. We then remove the solution and transfer the swollen soft PDMS slab to a partially sealed container, which allows the solvent to slowly evaporate for 24 hours at room temperature; fast evaporation results in the formation of cracks on the sample surface. The partially dried sample is then placed in a vacuum oven at 80°C overnight to ensure complete drying; the completion of the drying

process is further confirmed by monitoring the mass of soft PDMS slab over time, which does not decrease for longer heating periods. To confirm that the unreacted polymers have been completely removed, we compare the gel fraction measured by this gentle-swelling method to the standard Soxhlet extraction using acetone: *n*-hexane (50:50) (**Materials and Methods**). Indeed, the results are consistent with each other; for instance, for a soft PDMS elastomer with modulus of 20 kPa, the gel fraction measured using acetone: *n*-hexane (90:10) is 79.6% (wt/wt), which is in good agreement with the value, 80.3%, obtained by Soxhlet extraction.

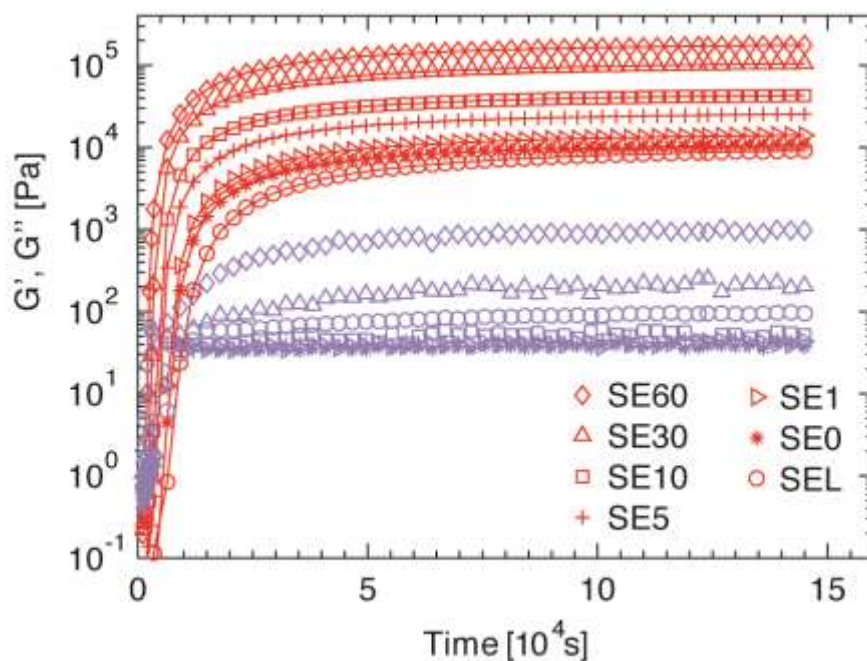
SI Figures

Figure S1. Dependence of viscoelastic properties of soft PDMS elastomers on curing time. Different symbols correspond to different samples (see **Table 1**); red and light blue represent shear storage (G') and loss (G'') moduli respectively. The moduli are measured at oscillatory shear frequency of 1Hz, temperature at 80°C, and constant strain of 0.5%.

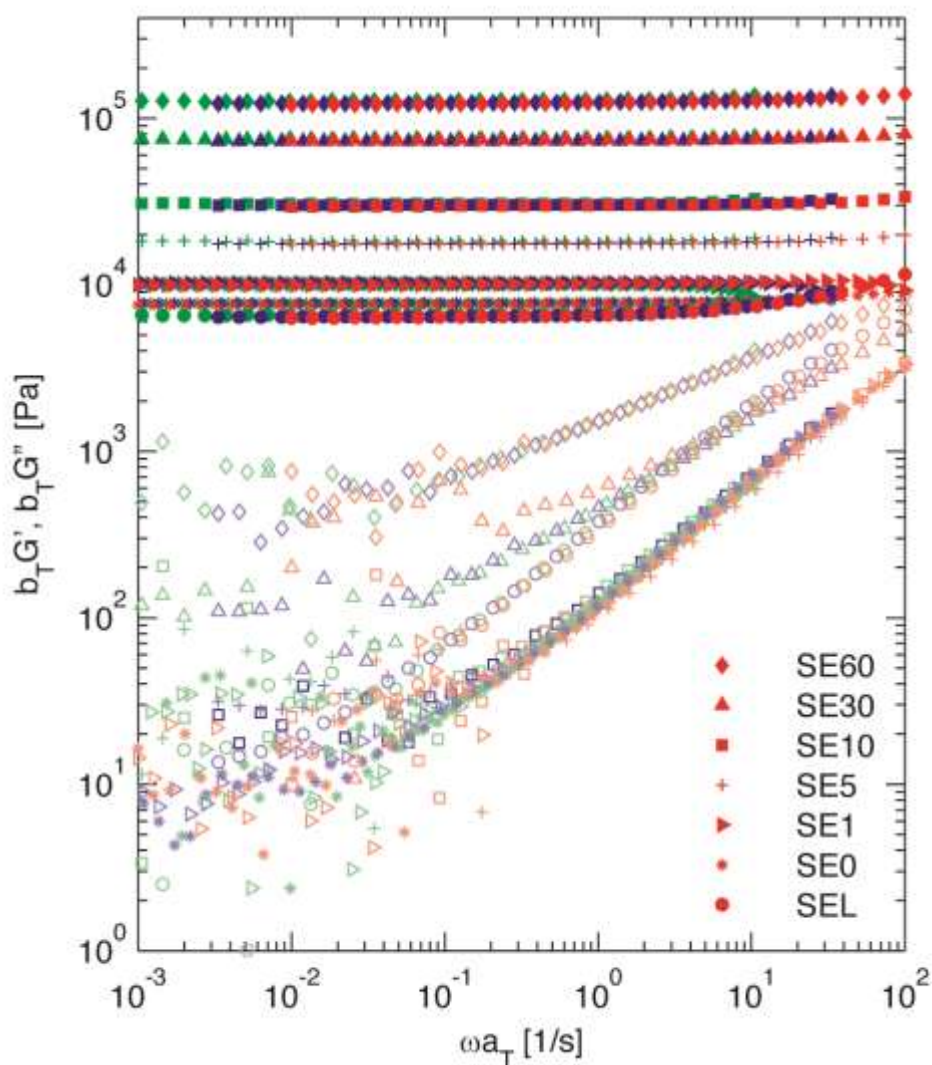


Figure S2. Time-temperature superposition curves for soft PDMS elastomers. Frequency dependence of storage (G' , filled symbols) and loss (G'' , empty symbols) for different samples obtained by classical time-temperature superposition shifts. The reference temperature is -20°C and the measurements were performed at -20°C (red), 20°C (blue) and 80°C (green). The shift parameters are the same for all samples: $a_T = 1/9.5$ for 20°C and $1/3$ for 80°C ; $b_T = 253/T$, in which T is the absolute temperature. Glass transition temperature for PDMS is about -20°C . Detailed recipe of each sample is listed in **Table 1**.

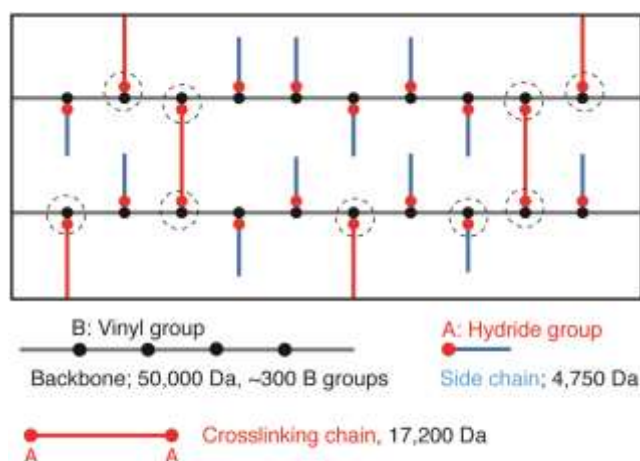


Figure S3. Elastically effective crosslinks and network strands in an unentangled polymer network. Dimmed black lines – backbone polymers, blue lines – side chains, red lines –crosslinking chains, black circles – vinyl groups, and red circles – hydride groups. A hydride group (red circle) react with a vinyl group (black circle) forming a crosslink. Only circled crosslinks and the network strands connecting them are elastically effective.

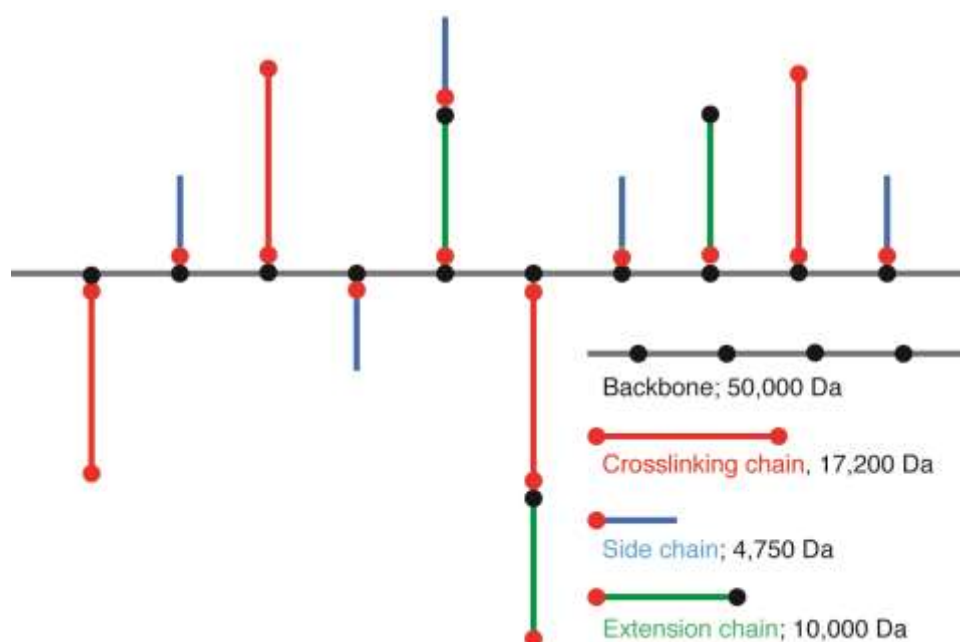


Figure S4. Effects of extension chains. An extension chain has its two ends functionalized differently, one with a hydride group (red circle) and the other with a vinyl group (black circle). The extension chain can directly graft to the backbone polymer, react with a short side chain forming a longer side chain that can as well graft to the backbone, react with a crosslinking chain to form a longer crosslinking chain, or react with another extension chain to form a longer extension chain.

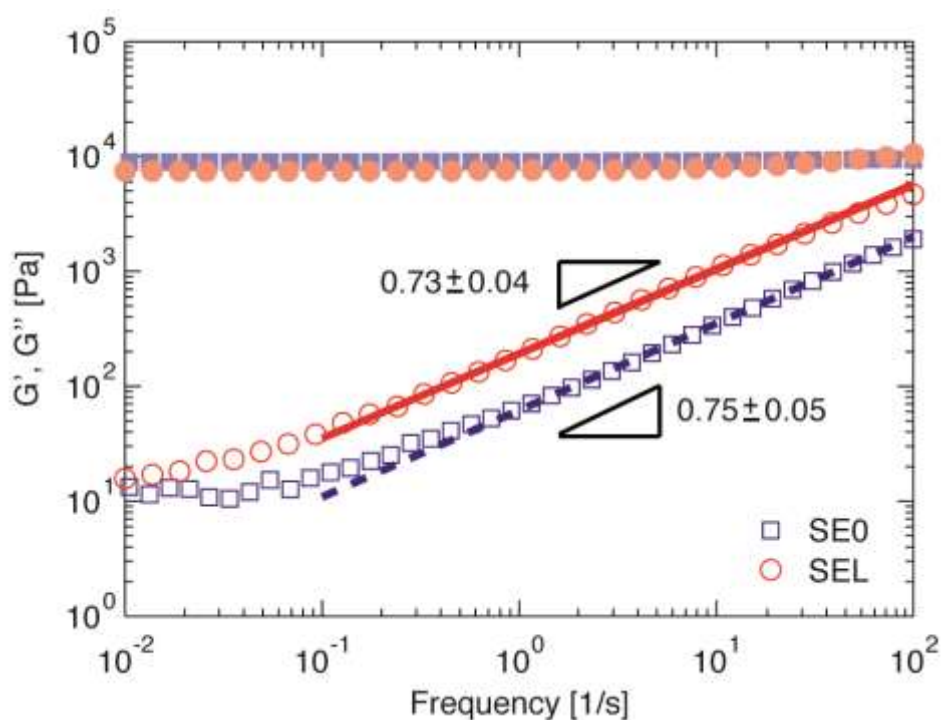


Figure S5. Control the loss moduli of soft PDMS elastomers. The moduli of soft elastomers formed by bottlebrush molecules with side chains of average molecular weight 4,750 g/mol (**SE0**) and 14,750 g/mol (**SEL**). In both samples the number of excess vinyl groups (reactive sites B) per bottlebrush molecule is the same. The loss modulus increases and is shifted up when the length of the side chains increases by 3 times from 4,750 g/mol to 14,750 g/mol, whereas the storage moduli are almost unchanged. The measurements are performed at constant strain of 0.5% and temperature at 20°C. Lines represent the best fits to logarithmic of the data points obtained at frequency >1Hz.

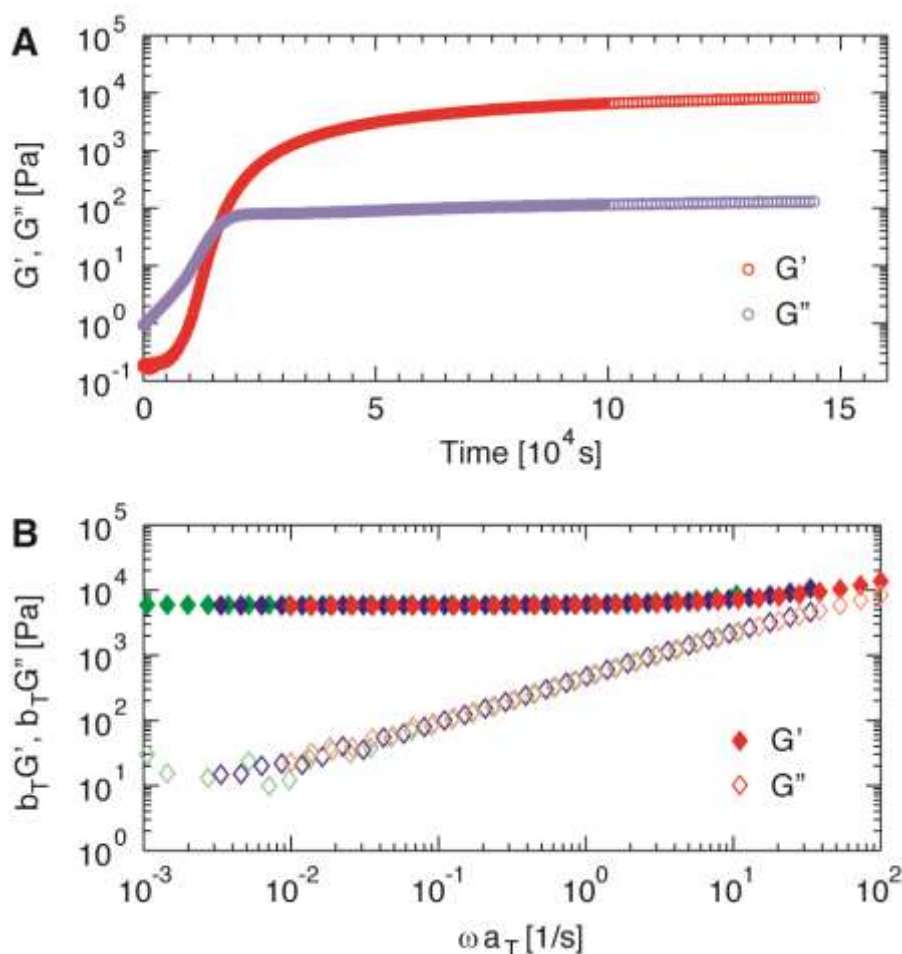


Figure S6. Quantification of the fraction of “impurities” in extension chains. The sample contains only *backbone polymers* and *chain extensions* with number ratio of 1:150. The chain extension is monovinyl-monohydride terminated polydimethylsiloxane, which has molecular weight of 10,000 g/mol and both ends functionalized differently, one carrying a reactive hydride site while the other carrying a reactive vinyl site. **(A)** Dependence of viscoelastic properties of the sample on polymerization time. **(B)** Classical time-temperature superposition curves for the sample. Frequency dependence of storage (G' , filled symbols) and loss (G'' , empty symbols) of different samples obtained by classical time-temperature superposition shifts. The reference temperature is -20°C and the measurements were performed at -20°C (red), 20°C (blue) and 80°C (green). The shift parameters are the same for all samples: $a_T = 1/9.5$ for 20°C and $1/3$ for 80°C ; $b_T = 253/T$, in which T is the absolute temperature.

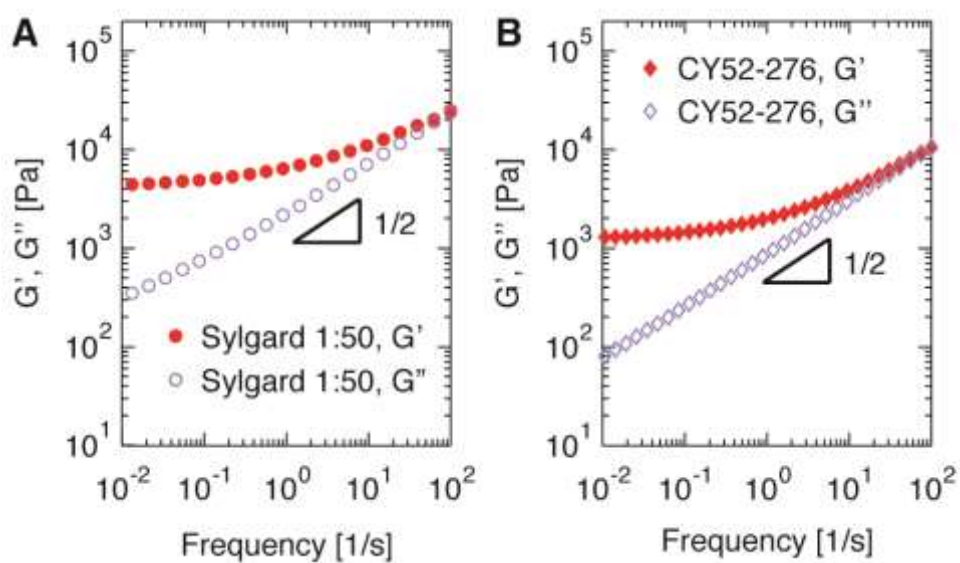


Figure S7. Viscoelastic properties of commercial PDMS products. Frequency dependence of storage (G' , filled symbols) and loss (G'' , empty symbols) for (A) Sylgard[®] 184 PDMS elastomers with curing agent/base mass ratio of 1:50 cured at 65°C for 6 hours and (B) Dow Corning silicone gel CY 52-276 cured at 70°C for 1 hour.

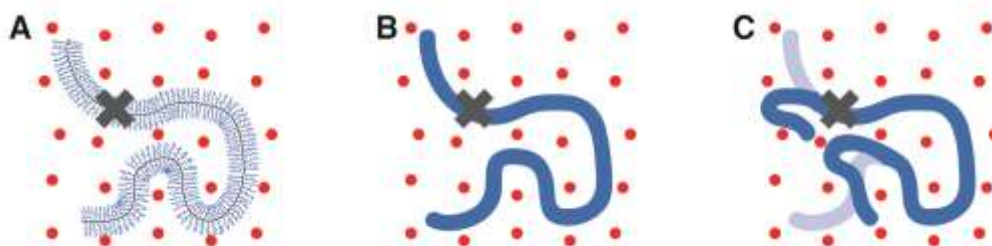


Figure S8. Illustration for the trapping of long dangling polymers in soft PDMS elastomers. (A) Many mono-functional chains (blue lines) dress up a multi-functional polymer into a hairy coat, forming a bottlebrush molecule. A bottlebrush molecule is linked to the network framework through a di-functional crosslinking chain (red line) and the rest reactive sites on the bottlebrush molecule are uncrosslinked; this process results in formation of long dangling ends. The attachment point is marked by the cross symbol. Red circles—obstacles representing confining meshes. (B) We model the bottlebrush molecule as an effective linear polymer with monomer size of the cross-section of the bottlebrush molecule. A dangling end cannot physically cross the obstacles; to relax, its dangling end has to retract from confining meshes sequentially. (C) Illustration of one step of the sequential relaxation process by retracting the dangling ends from constraining meshes. Dimmed lines represent the old position of the dangling ends, and the bright ones correspond to the new positions after retraction.

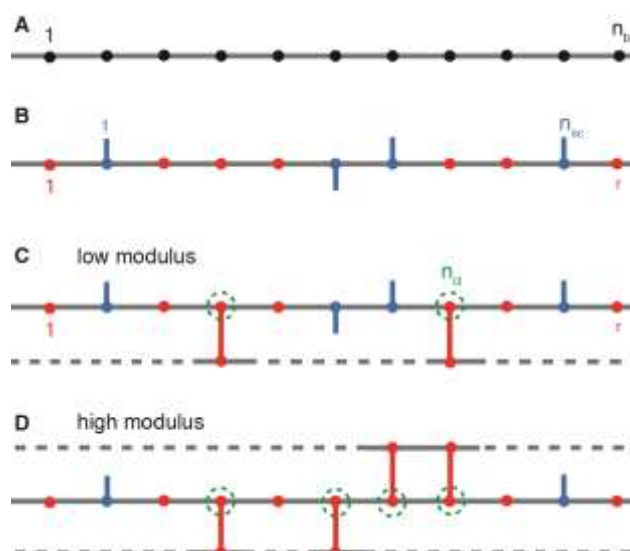


Figure S9. Unique crosslinking process for soft PDMS elastomers. (A) A precursor backbone polymer has n_b reactive sites. (B) During the formation of elastomers, n_{sc} of the reactive sites is used as grafting sites to attach side chains (blue dots and lines), and the remaining sites, $r = n_b - n_{sc}$, are available for crosslinking and called crosslinkable sites (red dots). (C) Among r crosslinkable sites, $2n_{cl}$ of them are crosslinked, as outlined by green circles; here n_{cl} is the number of crosslinking chains (red lines) per backbone polymer and factor 2 is due to the fact that each crosslinking chain reacts with two crosslinkable sites. The probability of a crosslinkable site being crosslinked is $q = 2n_{cl}/r$. (D) For the same number of reactive sites, the number of crosslinkable sites increases with network modulus, while the amount of side chains is reduced to release reactive sites for more crosslinking chains; this method ensures the same amount of sites react for samples of different moduli.

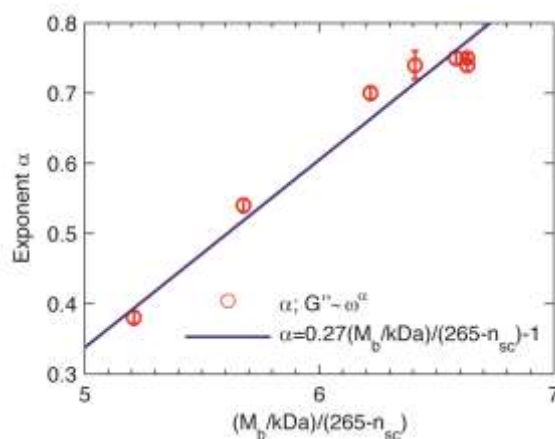


Figure S10. Dependence of the exponent, α , for the frequency dependence of loss modulus ($G'' \sim \omega^\alpha$) on reciprocal of the number of constraints per dangling polymer, $N_x/N_n \approx M_b/(n_b - n_{sc})$. Here M_b is the molecular weight of a bottlebrush molecule in the units of kDa. Symbols are the values of α determined from the best fits to loss modulus in the frequency range of 1—100Hz for different soft PDMS elastomer samples. Solid line represents the best fit to all the data points: $\alpha = 0.27 \frac{M_b}{\text{kDa}} \frac{1}{265 - n_{sc}} - 1$ (equation S11), and $n_b \approx 265$ corresponds to the number of reactive sites per multi-functional backbone polymer determined by the fitting.

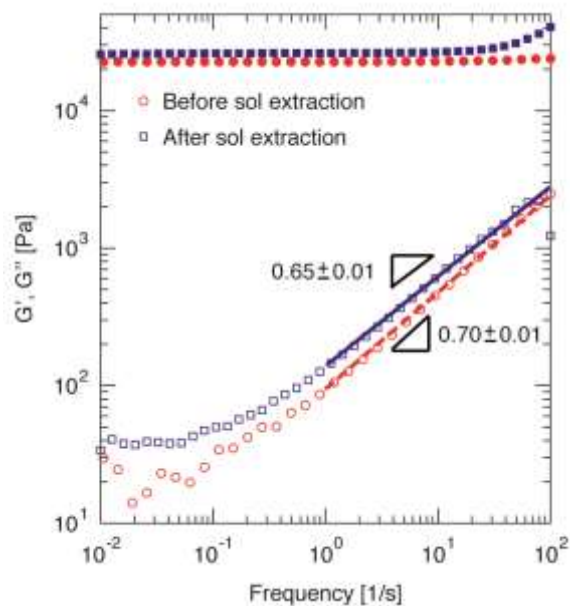


Figure S11. Effects of sol fraction on properties of soft PDMS elastomers. The viscoelastic properties of a soft PDMS elastomer sample before (circles) and after the sol extraction (squares): Fill symbols represent the shear storage modulus, G' , and empty ones correspond to shear loss modulus, G'' . Lines represent the best logarithmic fits to data points at frequency >1Hz. The amount of sol fraction in the sample is about 20% (wt/wt).

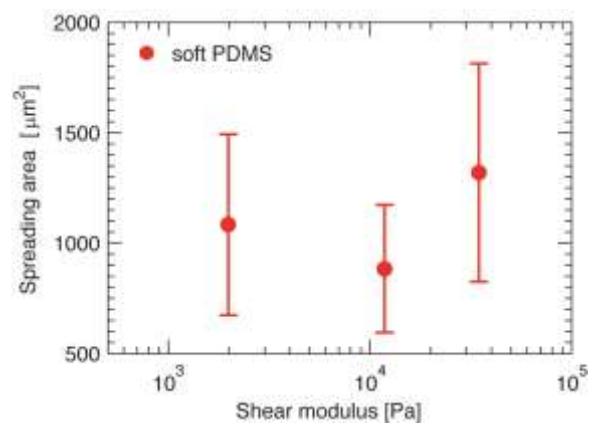


Figure S12. Spread area of isolated MDCK cells on substrates made of soft PDMS elastomers. Data are shown as mean \pm SD with the number of cells $n > 100$.

SI Tables

Curing agent/base ratio (wt/wt)	Modulus (kPa)	Gel fraction (wt%)
Sylgard [®] 1:10	1000	95.9
Sylgard [®] 1:20	270	87.7
Sylgard [®] 1:30	41	71.6
Sylgard [®] 1:50	4.5	53.4
Sylgard [®] 1:100	0.1	1.98
CY 52-276 1:1	1.4	59.2

Table S1. Recipe for fabrication of commercial silicone products. We use the Sylgard[®] 184 and CY 52-276 kits (Dow Corning, USA) to produce PDMS elastomers of different shear moduli by tuning the curing agent/base mass ratio. The gel fraction is measured using the Soxhlet extraction described in **Materials and Methods**.

SI Movies

Adhesion measurements for soft PDMS elastomers and commercial silicone products at separation rate of $v=1\mu\text{m/s}$.

Movie 1: SIMovie1_SoftPDMS_SE0_1ums.avi

Movie 2: SIMovie2_Sylgard1to50_1ums.avi

Movie 3: SIMovie3_CY52_276_1ums.avi

References

- [1] T. A. Kavassalis, J. Noolandi, *Phys Rev Lett* **1987**, 59, 2674.
- [2] M. Rubinstein, R. H. Colby, *Polymer Physics*, Oxford University Press, Oxford; New York **2003**.
- [3] J. E. Mark, *Physical Properties of Polymer Handbook*, Springer, New York **2006**.
- [4] M. Lang, M. Rubinstein, J. U. Sommer, *Acs Macro Lett* **2015**, 4, 177; D. Shirvanyants, S. Panyukov, Q. Liao, M. Rubinstein, *Macromolecules* **2008**, 41, 1475.
- [5] H. M. James, E. Guth, *J Chem Phys* **1943**, 11, 455.
- [6] D. S. Pearson, W. W. Graessley, *Macromolecules* **1978**, 11, 528.
- [7] P. G. d. Gennes, *Scaling Concepts in Polymer Physics*, Cornell University Press, **1979**.
- [8] J. G. Curro, P. Pincus, *Macromolecules* **1983**, 16, 559.